

1 A novel foaming additive derived from waste polyethylene 2 terephthalate (PET) for low-carbon warm mix asphalt

3
4 Fuliao Zou ^a, Ruiqi Chen ^a, Xiong Xu ^{b,c}, Jingting Lan ^a, Zhifei Tan ^a, Gaoyang Li ^a, Jiaqiu Xu ^a,
5 Xi Jiang ^a, Zhen Leng ^{a,*}

6
7 ^a Department of Civil and Environmental Engineering, The Hong Kong Polytechnic University,
8 Hung Hom, Kowloon, Hong Kong

9 ^b School of Civil Engineering and Architecture, Wuhan Institute of Technology, Wuhan, China

10 ^c Hubei Provincial Engineering Research Center for Green Civil Engineering Materials and
11 Structures, Wuhan, China

12

13 Abstract

14 Plastic pollution is growing relentlessly due to the careless disposal of waste plastic products. This
15 study focuses on converting waste plastic bottles into a foaming additive for the production of eco-
16 friendly warm mix asphalt (WMA). The additive, namely PET-TETA, was synthesized from waste
17 PET via an ammonolysis process. Its chemical and physical properties were characterized by X-
18 ray diffractometer (XRD), scanning electron microscope (SEM), and thermogravimetry-
19 differential thermal analyzer (TG-DTA) tests. The WMA mixture was prepared using PET-TETA
20 and compared to a conventional hot mix asphalt mixture and another WMA mixture prepared with
21 a commercial foaming additive. The performance of the asphalt mixtures was characterized using
22 the indirect tensile stiffness modulus test, moisture susceptibility test, and immersion Hamburg
23 wheel-tracking test. Results showed that PET-TETA was a semicrystalline material containing
24 approximately 26% hydration water, which could be released gradually during the preparation of
25 asphalt pavements. The overall performance of the WMA mixture with PET-TETA was
26 comparable to the other two asphalt mixtures, and it exhibited higher strengths and better resistance
27 to stripping. Therefore, PET-TETA can be considered a sustainable and effective WMA additive,
28 providing a solution to the issue of waste plastic disposal.

29 **Keywords:** Asphalt Pavement, Warm Mix Additive, Waste Plastic, Physical and Chemical
30 Properties

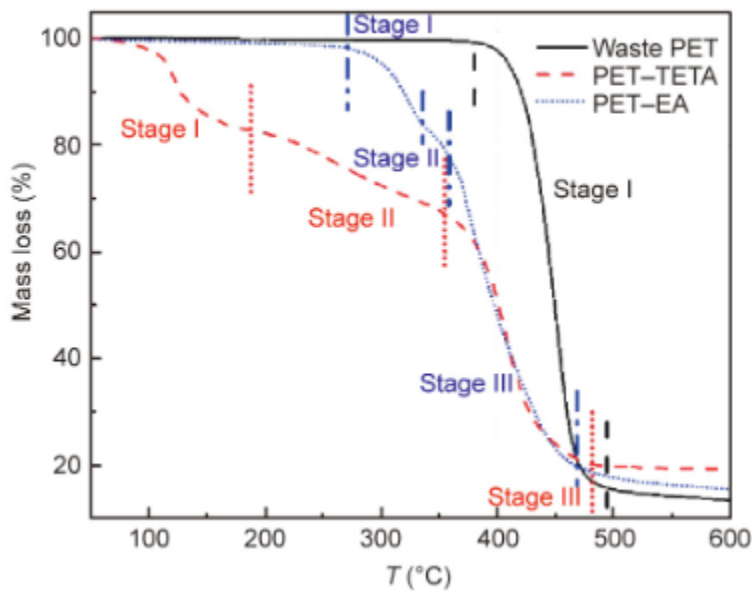
* * Corresponding Author (Email: zhen.leng@polyu.edu.hk)

31 **1. Introduction**

32 The ubiquitous presence of waste plastic has become one of the most pressing environmental
33 issues due to the increasing production of disposable plastic products over the last century. In Hong
34 Kong, waste plastic is the third largest constituent of municipal solid waste (MSW), with 945.9
35 thousand tons (21% of MSW) generated in 2020 alone (HK EPD, 2021). Although measures such
36 as the Plastic Recycling Pilot Scheme has been implemented by the local government to promote
37 plastic recycling, the capacity of the local recycling industry remains limited, and import policies
38 by other economies have become more stringent. As a result, only a small portion of waste plastic
39 is being recycled in Hong Kong. The amount of waste plastic recycled in Hong Kong was recorded
40 at 102 thousand tons in 2020, accounting for only 10.8% of the generated waste plastics. The vast
41 majority of waste plastics is disposed of at landfill sites. However, waste plastics are non-
42 degradable, posing significant environmental and economic challenges in a densely populated
43 urban city like Hong Kong.

44 Utilizing waste plastic in asphalt pavement as additives through chemical treatment is considered
45 a potential approach to address this problem. Previous studies have investigated the feasibility of
46 synthesizing beneficial additives from various waste plastics, including polyethylene (PE)
47 (Awwad and Shbeeb, 2007; Hınıslioğlu and Açar, 2004; Liang et al., 2021; Punith and
48 Veeraragavan, 2007), polyethylene terephthalate (PET) (Leng et al., 2018; Li et al., 2021; Sreeram
49 et al., 2018; Xu et al., 2022a; Xu et al., 2021), and polypropylene (PP) (Al-Hadidy and Tan, 2009;
50 Xu et al., 2022b; Yeh et al., 2005). Among them, PET derived additives have been thoroughly
51 studied and were thought to obtain the best potential for use in asphalt pavement. Li et al.
52 developed a method of using triethylenetetramine (TETA) and waste PET to synthesize a polymer
53 additive (i.e., PET-TETA) that improved the resistances to stripping and deformation of the

54 produced asphalt pavement (Li et al., 2021; Xu et al., 2021). It is interesting to note that PET-
55 TETA absorbed a certain amount of water through the hydration process during washing at the
56 final step for cleaning the product. **Fig. 1** illustrates the thermal property of PET-TETA. It can be
57 observed that the water of hydration is unstable and can be easily expelled by heating.
58 Approximately 20% of water was released in a temperature range of 100 – 200 °C, showing the
59 potential of PET-TETA to be used as a foaming additive in warm mix asphalt (WMA). This green
60 paving material-WMA allows conventional hot mix asphalt (HMA) to be mixed and paved at
61 lower temperatures without compromising on maintaining good engineering performance.



62

63 **Fig. 1.** Thermogravimetric analysis of waste PET and PET derived additives (Retrieved from Xu.
64 et al., 2021).

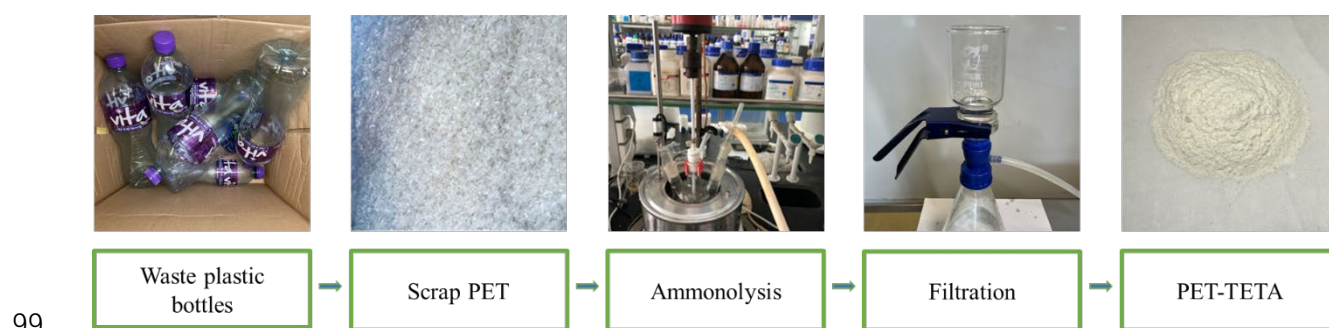
65 Foaming technologies have been widely used to prepare WMA due to their simple operation and
66 low construction cost, and the construction temperature can be reduced by 20-40 °C (Capitão et
67 al., 2012; Middleton and Forfyflow, 2009; Rubio et al., 2012; Zhang et al., 2018; Zou et al., 2022).

68 The foaming effect can be achieved by adding water-bearing agents or using water injection
69 techniques. A commercial product, aspha-min, has been commonly applied to prepare WMA in
70 practice. It is a synthetic zeolite that contains crystal water in its structure. When a water-bearing
71 agent is added to hot asphalt mixtures at construction temperatures of 140 -180 °C, the unstable
72 hydration water is detached and vaporized, which creates a rapid volume expansion of the asphalt
73 binder. This foaming effect improves the coating between asphalt binder and aggregate and allows
74 asphalt mixtures to be constructed at lower temperatures. Therefore, PET-TETA is considered an
75 environmental friendly alternative to the conventional commercial foaming additive due to its
76 comparable water-bearing property. However, the chemical and physical characteristics of PET-
77 TETA as a foaming additive have not been investigated yet. In addition, the performance of WMA
78 containing PET-TETA is needed to be studied. To fill this research gap, the objective of this study
79 is to investigate the performance of the WMA mixture prepared using PET-TETA through
80 comprehensive laboratory tests. The chemical and physical properties of the synthetic PET-TETA
81 were characterized by X-ray diffractometer (XRD), scanning electron microscope (SEM), and
82 thermogravimetry-differential thermal analyzer (TG-DTA) tests. The performance of the prepared
83 WMA mixture using PET-TETA was investigated through the indirect tensile stiffness modulus
84 test, moisture susceptibility test, and immersion Hamburg wheel-tracking test. The results were
85 compared to the conventional HMA mixture and another WMA mixture prepared with a
86 commercial foaming additive to validate the effectiveness of PET-TETA as a foaming agent in
87 asphalt pavement.

88 **2. Methodology**

89 **2.1. Synthesis and characterization of PET-TETA additive**

90 In this study, waste PET water bottles were collected from local plastic recycling bins. A
91 pretreatment process was conducted to eliminate impurities by removing product labels and
92 washing the bottles using normal detergent solutions and water. Waste PET bottles were then cut
93 into rod-like pieces with an approximate length of 5 mm, and dried at 80 °C for 4 hours. Afterward,
94 the PET waste was added to a round bottom flask with TETA, and the mass ratio of PET and
95 TETA was adjusted to 1:2. The ammonolysis process of PET was performed under reflux at 140
96 °C for 2 hours. Synthetic products were collected at the end of the reaction using vacuum filtration.
97 The PET-TETA additive, a white powder, was obtained through water cleaning, drying, and
98 grinding processes. **Fig. 2** illustrates the synthesis process of PET-TETA.



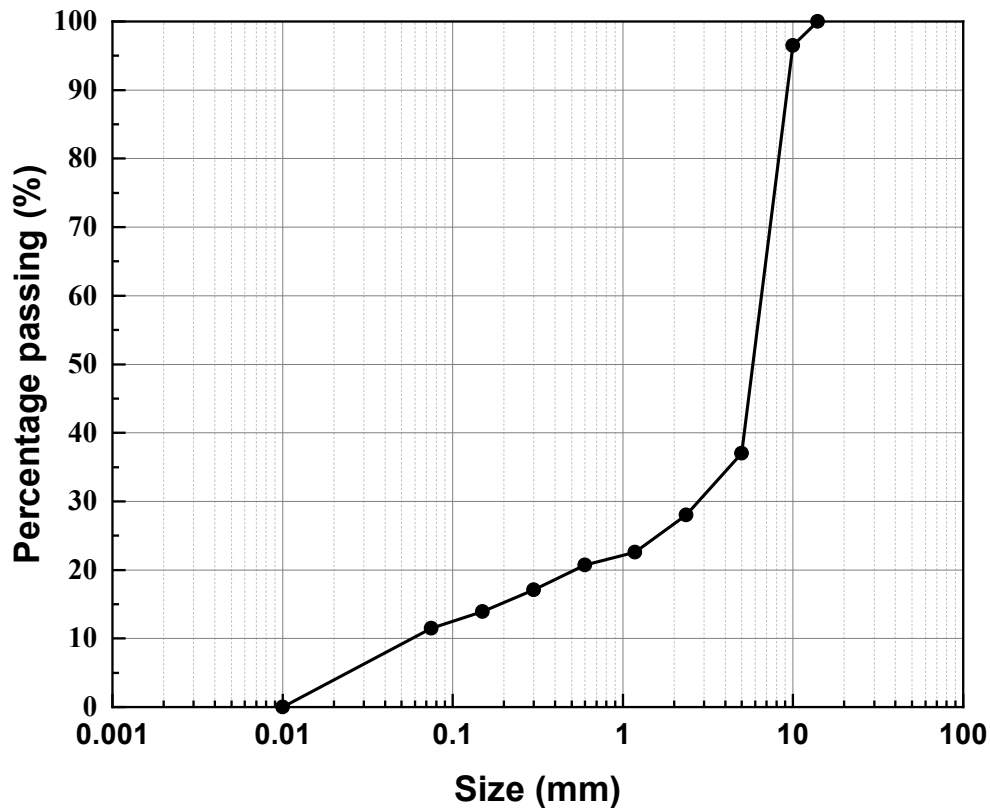
100 **Fig. 2.** Synthesis process of PET-TETA from waste plastic bottles

101 The properties of the two WMA additives (i.e., PET-TETA and aspha-min) were characterized by
102 XRD, SEM, and TG-DTA tests. The XRD test was conducted using a Rigaku SmartLab X-ray
103 diffractometer with a 9-kW rotating anode X-ray source and a high-energy resolution
104 semiconductor detector. The scanning was operated using a step width of 0.02 °, a speed of 4 °
105 /min, and an X-ray wavelength (λ) of 1.54 Å. The detected XRD patterns were compared with the
106 powder diffraction file (PDF) database for identification. The SEM test was conducted using a
107 Tescan VEGA3 SEM system with a high spatial resolution (up to 100,000X) with a secondary

108 electron and backscatter detector. The TG-DTA test was conducted using a Rigaka Thermo plus
109 EVO2 thermal analyzer. The measured temperature range was set from 25 °C to 600 °C with a
110 heating rate of 10 °C/ min.

111 **2.2. Raw materials and sample preparation**

112 Three asphalt mixtures were prepared in this study, including conventional hot mix asphalt
113 (HMA), WMA with PET-TETA (PET), and WMA with aspha-min (APM). The dosage of PET-
114 TETA was 2% by the mass of the asphalt binder according to previous studies. The dosage of
115 aspha-min was 5% by the mass of the asphalt binder based on supplier recommendations. A
116 frequently used surface course material for local carriageway pavements, namely polymer-
117 modified stone mastic asphalt with a nominal maximum aggregate size of 10 mm (PMSMA10),
118 served as the mixture design for all three types of mixtures (Highways Department, 2016). The
119 coarse aggregates, fine aggregates, and mineral fillers used in this study were local granite rocks.
120 The asphalt binder used in this study was styrene-butadiene-styrene (SBS) polymer-modified
121 bitumen with a Superpave performance grade of PG76-16 (AASHTO, 2013a). The binder content
122 was set at 6.0% by the total mass of the asphalt mixture (the same hereinafter, if not specified).
123 Hydrated lime and cellulose fiber were also used in this study, and their contents were 0.3% and
124 2%, respectively. **Fig. 3** illustrates the gradation curve of the PMSMA10 mixture.



126

127

Fig. 3. Aggregate gradation of the PMSMA10 mixture.

128

129

130

131

132

133

134

Superpave gyratory compactor (SGC) was adopted in this study to prepare test specimens. The mixing temperatures of HMA mixtures and WMA mixtures were controlled at 180 °C and 155 °C, and their compaction temperatures were controlled at 160 °C and 135 °C to achieve a construction temperature reduction of 25 °C. In the preparation of WMA mixtures, the foaming of asphalt binder was achieved by shear-mixing the foaming additive into the hot asphalt binder at 155 °C for 3 minutes. The foamed asphalt binder was subsequently mixed with the aggregates and the mixture was compacted at the designed temperature. The mixtures were compacted to a designed air void

135 content of $4\% \pm 0.5\%$ and tested for indirect tensile stiffness modulus (ITSM). Specimens with a
136 higher air void content of $7\% \pm 0.5\%$ were also produced for the moisture susceptibility test and
137 Hamburg wheel-tracking test according to test specifications. Specimens were made in two
138 replicates for Hamburg wheel-tracking test, while four replicates were tested for the other tests.
139 **Table 1** presents the general information on the prepared specimens and engineering tests.

140 **2.3. Laboratory tests for asphalt pavement performances**

141 Surface distresses, such as rutting, moisture damage, fatigue cracking, and thermal cracking are
142 often generated after repetitive traffic loading (Jiang et al., 2022; Li et al., 2020; Tan et al., 2022).
143 The high temperature performance and intermediate temperature durability of the produced asphalt
144 mixtures were investigated in this study regarding the relatively hot climate of Hong Kong. In
145 addition, the moisture susceptibility of the prepared WMA mixtures was evaluated concerning the
146 water introduction during the foaming process (Hasan et al., 2015; Xu et al., 2017). The cracking
147 resistance of HMA, PET, and APM at intermediate temperatures was evaluated by the ITSM test.
148 The rutting resistance of HMA, PET, and APM at high temperatures was investigated by
149 immersion Hamburg wheel-tracking test. The moisture damage resistance of HMA, PET, and
150 APM was determined by the moisture susceptibility test with freeze-thaw cycle conditioning.

151 The dimensions of the test specimens produced for the ITSM test were 100 mm (diameter) \times 40
152 mm (height) (BSI, 1993). To investigate the cracking performance of the prepared mixtures right
153 after the construction and after a long service time, the produced specimens were subjected to a
154 short-term and long-term aging process. The laboratory aging process was conducted in the
155 following ways: before compaction, loose mixtures were conditioned at 135 °C for 4 hours in a
156 force-draft oven; after compaction, compacted mixtures were further aged at 85 °C for 5 days in

157 the oven (AASHTO, 2010). A PAVETEST dynamic testing system (DTS-30) was used to measure
 158 the modulus of HMA, PET, and APM.

159 The dimensions of the test specimens produced for the moisture susceptibility test were 100 mm
 160 (d) × 62.5 mm (h) (ASTM, 2014). The moisture susceptibility was evaluated by the Tensile
 161 strength ratio (TSR) between freeze-thaw cycle conditioned mixtures and unconditioned mixtures.
 162 The conditioning process was conducted by saturating the prepared specimens with water. Then,
 163 the partially saturated specimens (i.e., 70% to 80%) were conditioned at -18 °C for 16 h in a freezer
 164 and 60 °C for 24 h in a water bath. The indirect tensile (IDT) strength of the produced asphalt
 165 mixtures was measured by DTS-30.

166 The dimensions of the test specimens produced for the Hamburg wheel-tracking test were 150 mm
 167 (d) × 60 mm (h) (AASHTO, 2013b). A CRT-WTIM wheel tracker (Cooper Research Technology)
 168 with linear variable differential transformers (LVDTs), a water bath with a temperature control
 169 system, and two moving steel wheels was used to record the rut depth in this study. The immersion
 170 Hamburg wheel-tracking test was conducted using a wheel load of 705 N and a rolling speed of
 171 52 passes/ min. The test specimens were conditioned and tested in the water bath at 50 °C, the
 172 most common temperature used for the test. Rut depth was recorded every 200 passes, and the test
 173 was completed after 20,000 passes or a maximum LVDT displacement of 1.6 in. (40.9 mm).

174 **Table 1** Details of the prepared specimens and engineering tests.

Label	HMA	APM	PET
Mixture	Conventional hot mix asphalt	Warm mix asphalt with aspha-min	Warm mix asphalt with PET-TETA
Mixing/ compaction temperature (°C)	180/ 160	155/ 135	155/ 135

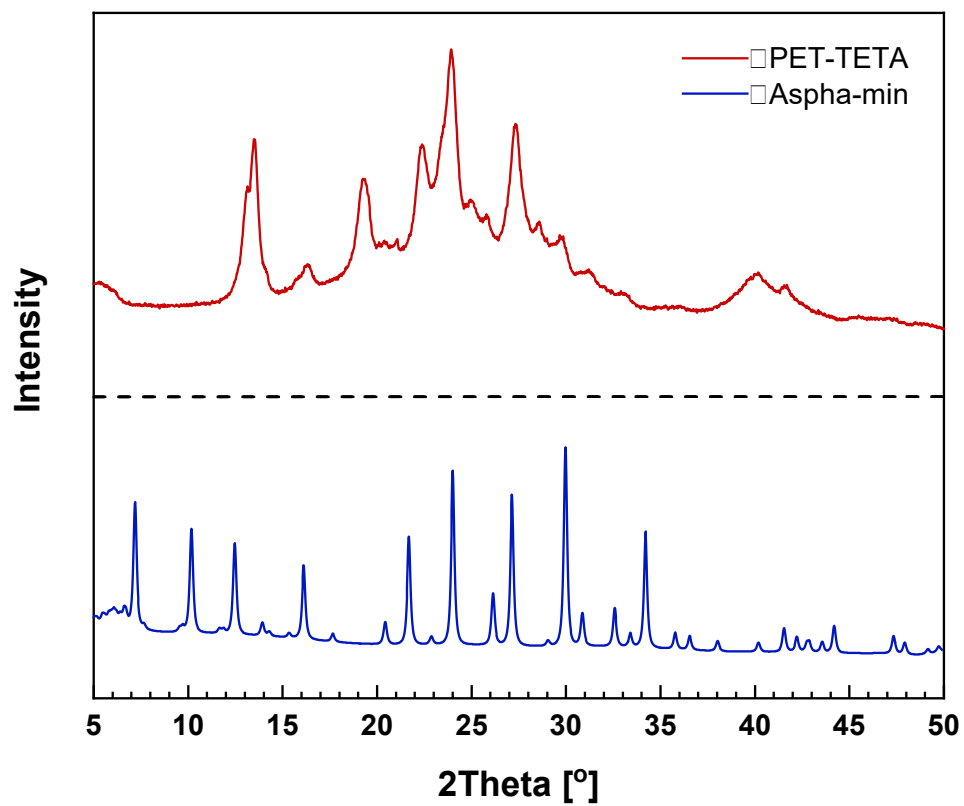
Test	Indirect tensile stiffness modulus test
Specimen diameter/ thickness (mm)	100/ 40
Air void content (%)	3.5 - 4.5
Test temperature (°C)	20 ± 0.2
Test	Moisture susceptibility test
Specimen diameter/ thickness (mm)	100/ 62.5
Air void content (%)	6.5 - 7.5
Test temperature (°C)	25 ± 0.5
Test	Hamburg wheel-tracking test
Specimen diameter/ thickness (mm)	150/ 60
Air void content (%)	6.5 - 7.5
Test temperature (°C)	50 ± 1.0

175 **3. Results and Discussion**

176 **3.1. Characterization of PET-TETA**

177 **Fig. 4** illustrates the XRD patterns of PET-TETA and aspha-min. A clear crystalline structure can
178 be observed for aspha-min. However, PET-TETA behaved more like an amorphous polymer but
179 also contained a few crystalline regions. The crystalline phase of zeolite A was identified in aspha-
180 min based on the PDF database. Aspha-min captures hydration water in its tight polyhedral cage
181 crystalline structure, where the water molecules are linked by coordinate covalent bonds or
182 hydrogen bonds. However, it was unable to match PET-TETA to any specific crystals as it exhibits
183 no apparent crystalline structure, indicating that the mechanisms of absorbing and releasing water
184 are quite different for PET-TETA and aspha-min. The results of XRD patterns show that PET-
185 TETA has both crystalline regions and amorphous regions. Unlike aspha-min that stores hydration
186 water in its crystalline structure, the crystalline region in PET-TETA genuinely has an adverse

187 effect on water absorption. The crystalline region is the area of molecules where polymer chains
188 are more aligned and closer to each other. The amorphous region is the area of molecules where
189 polymer chains are loosely distributed, and there is no orderly manner. PET-TETA absorbs water
190 through hydrogen bonding with water molecules, each hydrophilic amide group in PET-TETA has
191 a slightly positive hydrogen atom and two lone pairs on the oxygen atom, which both can engage
192 in hydrogen bonding with water molecules, and both hydrogen bonding networks extend in all
193 directions. The molecules in crystalline regions are stacked together and held by the van der Waals
194 force, making it difficult for water molecules to attach within these regions. However, the
195 amorphous regions in PET-TETA grant it the ability to bond with water molecules as there is more
196 space for water molecules to be absorbed instead of the crystalline regions. **Fig. 5** shows a
197 schematic diagram of the crystalline and amorphous regions of PET-TETA. Most chains in PET-
198 TETA are randomly coiled and entangled in a disordered pattern, while some chains are aligned
199 together and form an ordered structure.

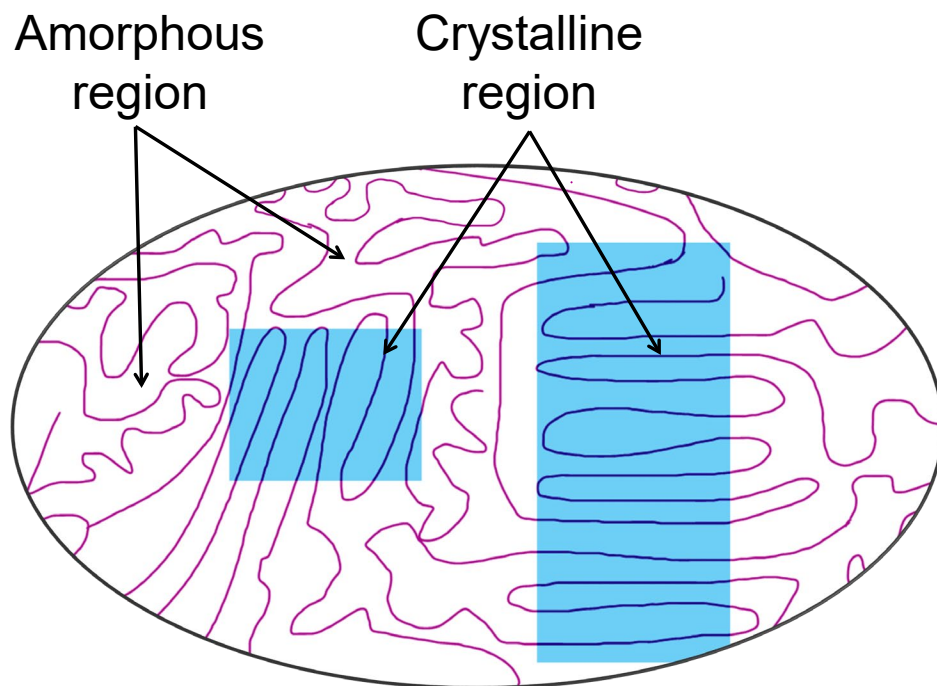


200

201

Fig. 4. XRD patterns of PET-TETA and aspha-min.

202



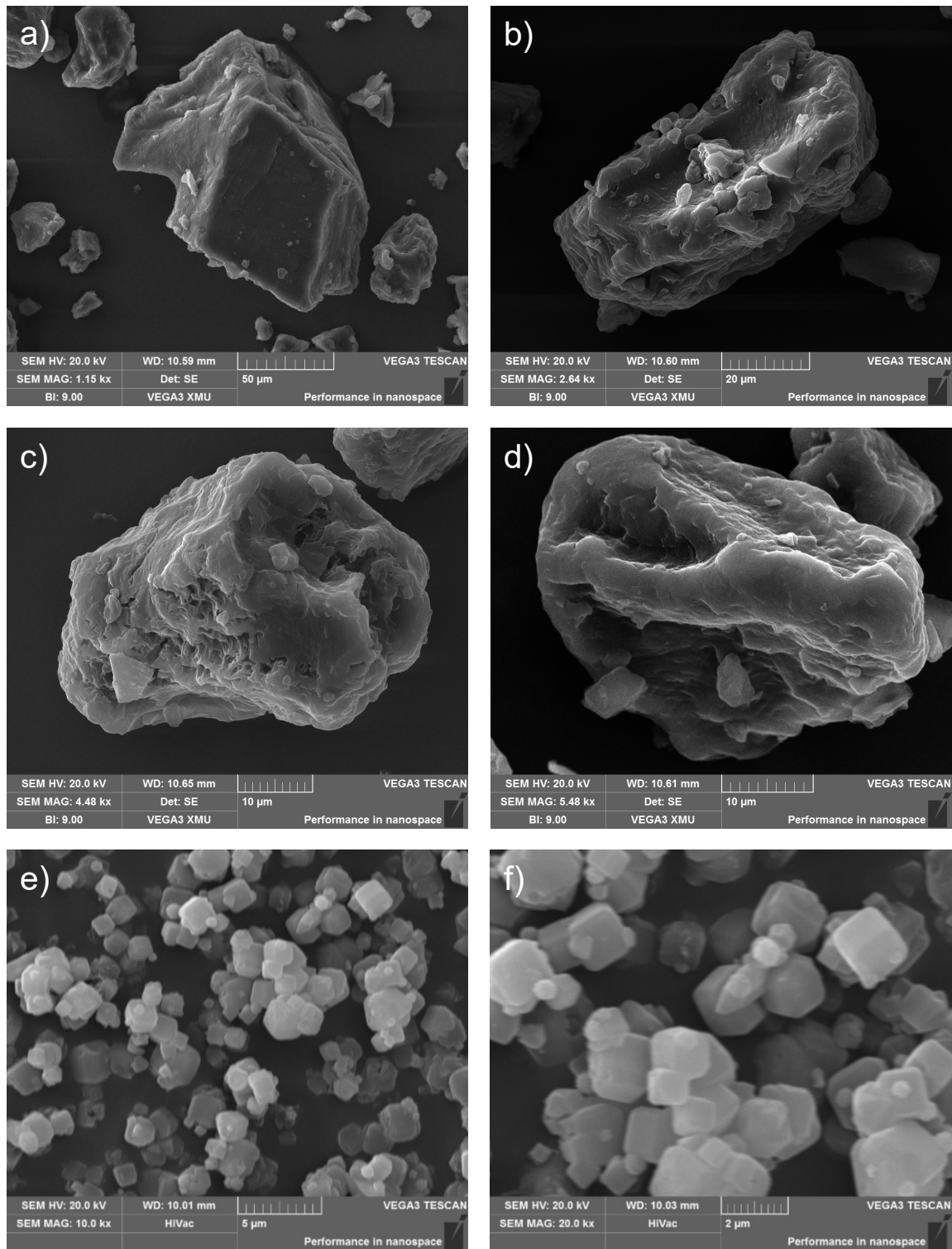
203

204 **Fig. 5.** Schematic diagram of PET-TETA that contains both amorphous and crystalline regions.

205 **Fig. 6** shows the SEM images of PET-TETA and aspha-min. It is clear to observe the cubic
 206 crystalline structure of aspha-min from **Fig. 6 (e) and (f)**, and the crystalline size is about $2\mu\text{m}$ in
 207 diameter. However, PET-TETA presents random morphologies and poses no specific grain sizes.
 208 The crystalline regions of PET-TETA can be observed in **Fig. 6 (a)**, which form a trapezoidal
 209 prism-like structure. The molecules in crystalline regions sit together in a more ordered pattern,
 210 and the chains are stacked together so that the structure displays flat surfaces and sharp edges.

211 In contrast, **Fig. 6 (b), (c), and (d)** present poorly defined patterns of amorphous regions since
 212 their components are in irregular arrangement, showing rough surfaces and round edges. In
 213 addition, a lot of pores are observed in the structures from the SEM images. The disordered
 214 arrangement of molecule chains in amorphous regions creates voids in their structures, which helps
 215 PET-TETA to absorb water by allowing water molecules to fit in these spaces. The particle sizes

216 of PET-TETA ranged from several micrometers to hundreds of micrometers, and bigger particles
217 had more crystalline patterns, while finer particles presented more amorphous structures. Unlike
218 the ordered molecules in crystalline regions, amorphous regions contain no plane of atoms that can
219 slip past each other, and the stress is not relieved during the grinding process. Therefore, excessive
220 stress formed cracks at amorphous regions, and the molecule chains were broken up into small
221 pieces, while the molecules in crystalline regions could generally maintain their structures,
222 resulting in their size differences.



223

224 **Fig. 6.** SEM images of PET-TETA ((a) 1k \times , (b) 3k \times , (c) 4k \times , (d) 5k \times) and aspha-min ((e) 10k \times

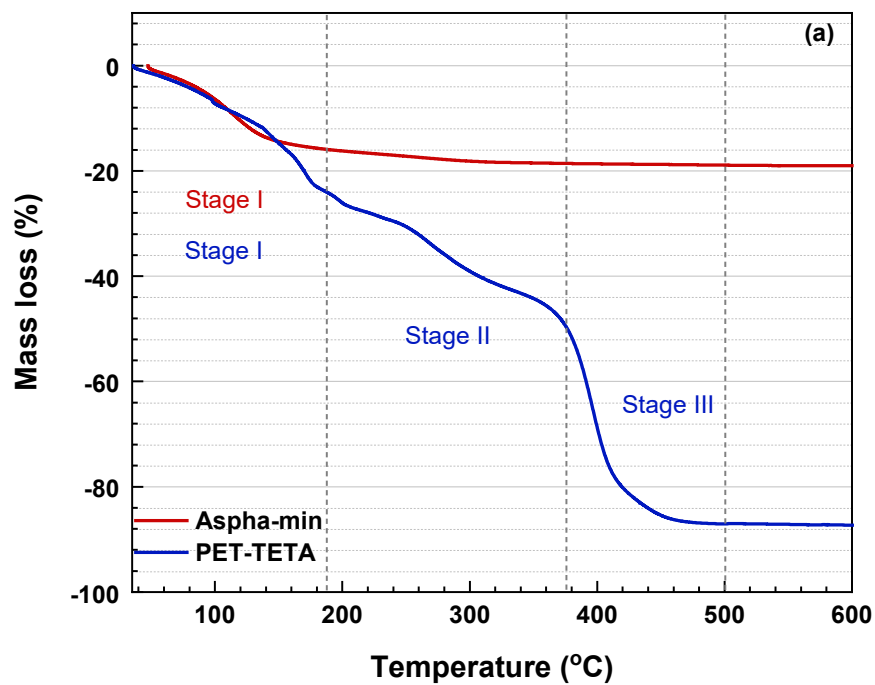
225

and (f) 20k \times)

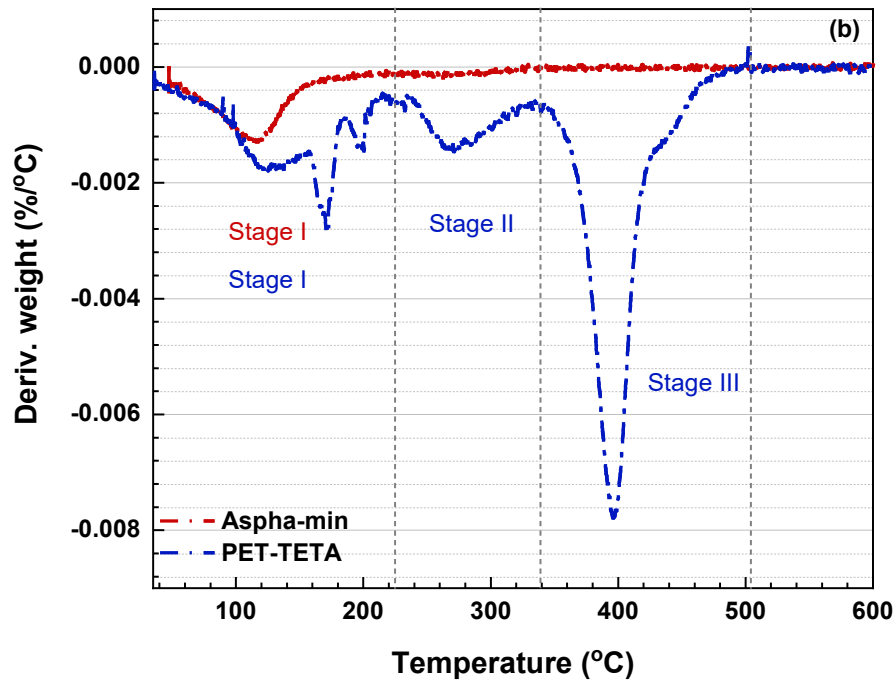
226 **Fig. 7** shows the thermal properties of PET-TETA and aspha-min. The mass loss before 200 °C
227 indicates the release of water, and the mass loss over the range of 200-600 °C implies the release
228 of pyrolysis products by thermal decomposition (Duan et al., 2008; Saldo et al., 2002). It can be
229 observed that both materials released hydration water when the temperature started to increase,
230 but aspha-min had only one stage of mass loss while PET-TETA presented multiple stages of mass
231 loss. The total mass losses of aspha-min and PET-TETA at 600 °C were 18.7% and 87.9%. The
232 results suggest that aspha-min has no thermal decomposition except for the release of crystal water,
233 while PET-TETA has components that can be decomposed at high temperatures. Aspha-min, a
234 hydrated aluminosilicate zeolite, released crystal water when heating began and continued up to
235 approximately 200 °C. Then, it decomposed very slowly when the temperature kept rising from
236 200 °C to 600 °C since aluminosilicate is relatively stable and hardly decomposes under such
237 temperatures. However, PET-TETA, the ammonolysis product of PET, also released hydration
238 water when the temperature increased, but it further degraded at about 250 °C and 400 °C. The
239 observed percentage mass losses of hydration water from aspha-min and PET-TETA were 16.3%
240 and 26.0%, which implies that PET-TETA has better water bonding abilities than aspha-min.

241 Moreover, the earlier heat absorption peak of aspha-min (i.e., about 110 °C) indicates that aspha-
242 min is more sensitive to temperature changes than PET-TETA, which had a heat absorption peak
243 at approximately 150 to 170 °C. Based on the thermal properties of the two materials, PET-TETA
244 is expected to have a better foaming effect and asphalt coating by releasing more hydration water
245 and preserving steadier water evaporations at high construction temperatures. **Fig. 8** shows the
246 foaming effect of aspha-min and PET-TETA in asphalt binder at 150 °C. It can be clearly observed
247 that PET-TETA performed better foaming. PET-TETA generated large bubbles, while aspha-min
248 produced small dense foams. The differences in their water bonding characteristics might be the

249 major reason for it. PET-TETA contains larger amounts of hydration water that is mostly bonded
250 to the molecules in the loose amorphous region, which is preferred to be released when there is
251 sufficient heat. However, aspha-min encloses less hydration water, and it is caged in the tight
252 polyhedral crystalline structure. Therefore, it released less water in the foaming process, and the
253 escape of water was slower, resulting in inferior foaming compared to PET-TETA.



254



255

256

Fig. 7. (a) weight loss and (b) heat flow of aspha-min and PET-TETA.

257



258

259

Fig. 8. Foaming effect of (a) aspha-min and (b) PET-TETA.

260

3.2. Indirect tensile stiffness modulus of the produced asphalt mixtures

261

Fig. 9 presents the ITSM test results of HMA, PET, and APM. The indirect stiffness modulus was measured at 2,371 MPa, 2,707 MPa, and 2,148 MPa for unaged HMA, PET, and APM, respectively. WMA mixtures generally have lower stiffness moduli than HMA mixtures because they suffered lower aging during the manufacturing process with reduced production temperatures, as observed in the case of APM. However, PET showed the highest stiffness modulus that was 14% higher than HMA and 26% higher than APM. It was due to the increased bonding strength between PET modified asphalt binder and mineral aggregate. PET-TETA composes amino groups that can form hydrogen bonds with the surface hydroxyl groups of aggregate. Besides, the alkaline amino groups of PET-TETA can interact with aggregate granite, which is a typical acidic rock. Therefore, PET has a higher resistance to elastic deformation because of its stronger molecular bonding, resulting in an increased stiffness modulus.

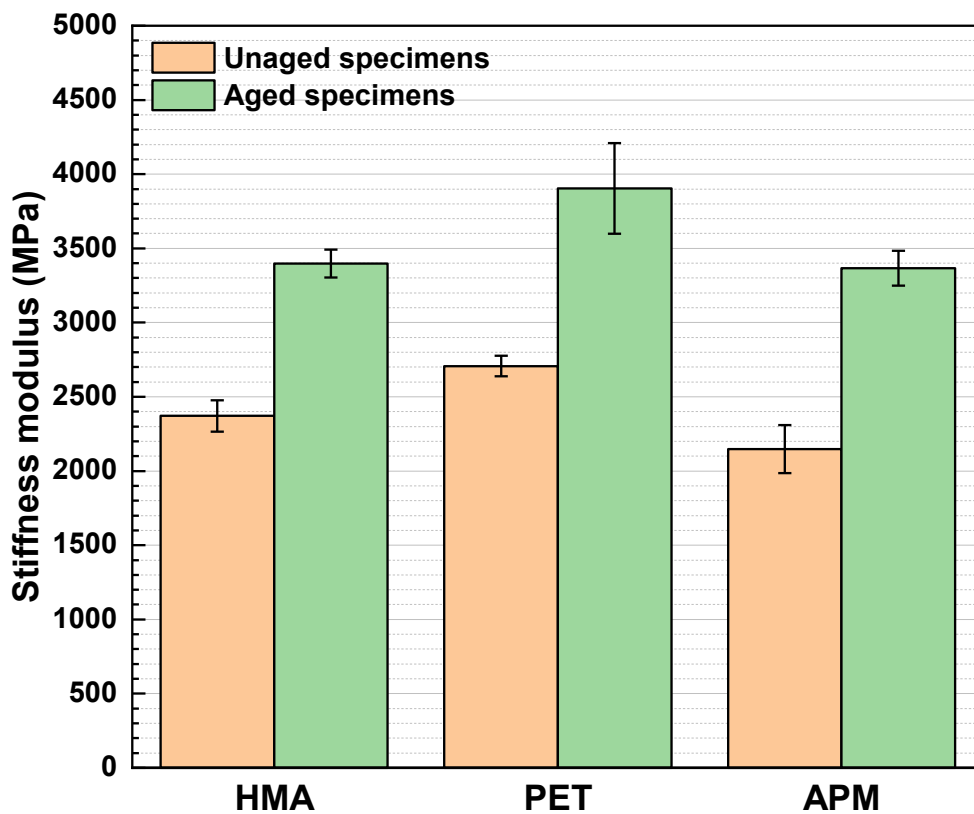
271

272

The indirect stiffness modulus was measured at 3398 MPa, 3904 MPa, and 3367 MPa for long-term aged HMA, PET, and APM, respectively. The differences in the values of the indirect stiffness moduli before and after the long-term aging process were 1026 MPa for HMA, 1197 MPa for PET, and 1218 MPa for APM, indicating that the three asphalt mixtures have similar resistances to aging. After long-term aging, PET still presented the highest stiffness modulus, which was approximately 15% higher than that of HMA and APM. The findings of the ITSM test suggest that the use of aspha-min, a zeolite based foaming additive, had little influence on the stiffness modulus of the material, and it could hardly affect the long-term cracking resistance of the produced asphalt mixture. The zeolite based foaming additive could only create a foaming effect by releasing crystal water, but the material itself can not react with asphalt binder so that it presents insignificant effects

281

282 on the stiffness modulus of the produced asphalt mixture. However, the application of PET-TETA
283 could influence the stiffness modulus of the produced asphalt material through the modification of
284 asphalt binder and improve its interaction with aggregate. As a result, PET performs better
285 resistance to elastic deformation. However, it may also have a higher sensitivity to cracking caused
286 by plastic deformation at intermediate temperatures.



287

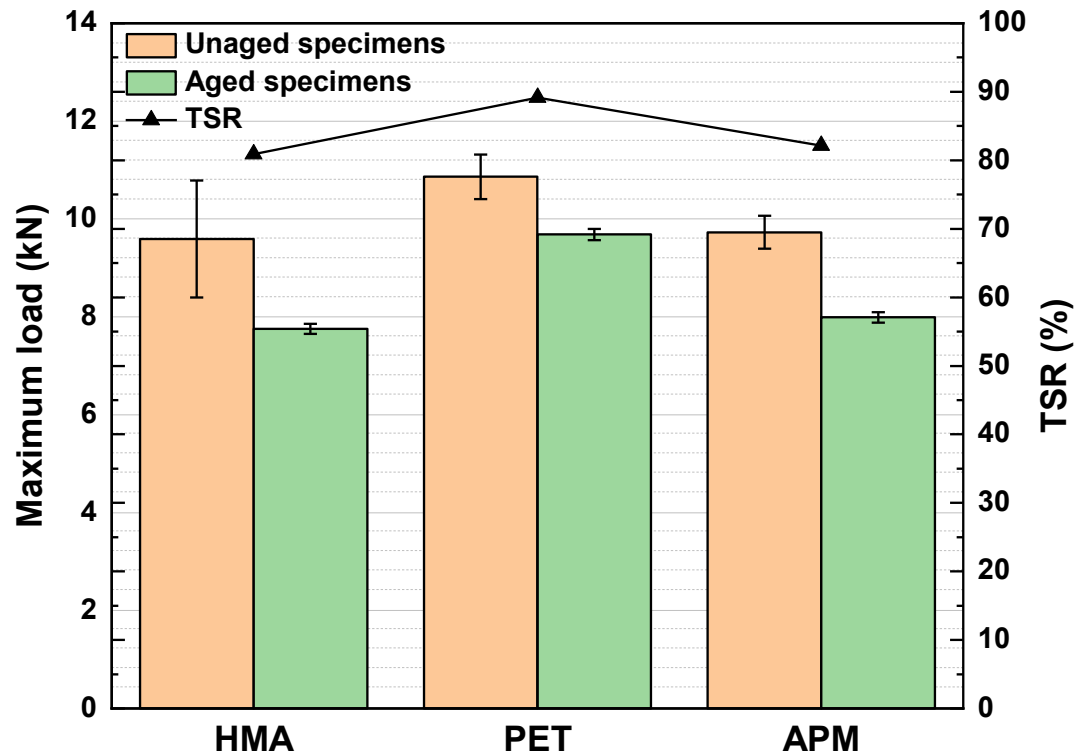
288 **Fig. 9.** ITSM test results of the produced asphalt mixtures before and after aging

289 3.3. Susceptibility to moisture damage of the produced asphalt mixtures

290 The moisture susceptibility of asphalt mixtures was investigated by measuring the indirect tensile
291 (IDT) strengths of samples before and after the freeze-thaw cycle conditioning. The results of the

292 IDT strengths of HMA, PET, and APM are illustrated in **Fig. 10**. It can be observed that PET had
293 the highest IDT strength among the three mixtures regardless of the water conditioning. Before
294 conditioning, HMA, PET, and APM showed IDT strengths of 9.6 kN, 10.9 kN, and 9.7 kN,
295 respectively. After conditioning, the IDT strengths of all three mixtures were decreased due to
296 moisture damage, with values recorded at 7.8 kN, 9.7 kN, and 8.0 kN for HMA, PET, and APM,
297 respectively. The IDT strength of HMA and APM was comparable to each other, which suggests
298 that the application of aspha-min had insignificant influences on moisture susceptibility.

299 However, the use of PET-TETA improved the IDT strength of the produced asphalt mixture. PET
300 displayed IDT strengths of about 13% and 23% higher than the other two asphalt mixtures in dry
301 and wet conditions. Moreover, PET had the highest tensile strength ratio (TSR) of 89.2%, while
302 the TSR values for HMA and APM were 80.9% and 82.1%, respectively. The results suggested
303 that the produced WMA mixtures had no moisture damage concerns compared to the conventional
304 HMA. Moreover, the application of PET-TETA could significantly reduce the susceptibility to
305 moisture damage of the produced asphalt mixture. The increase in the bonding strength and the
306 resistance to water damage by using PET-TETA was mainly due to the following reasons: 1) The
307 higher polarity of PET-TETA made the modified bitumen more affiliated to the polar aggregate
308 surface, resulting in a better coating; 2) PET-TETA composes amino groups that could form strong
309 hydrogen bonds with the surface hydroxyl groups of aggregate; 3) The alkaline amino groups of
310 PET-TETA could interact with the acidic aggregate granite that was used in this study; 4) Water
311 is more likely to attack the aggregate surface due to the hydrophilic nature of the mineral aggregate,
312 the increased adhesion between PET-TETA modified bitumen and aggregate prevents the adhesive
313 failure caused by water damage.



314

315

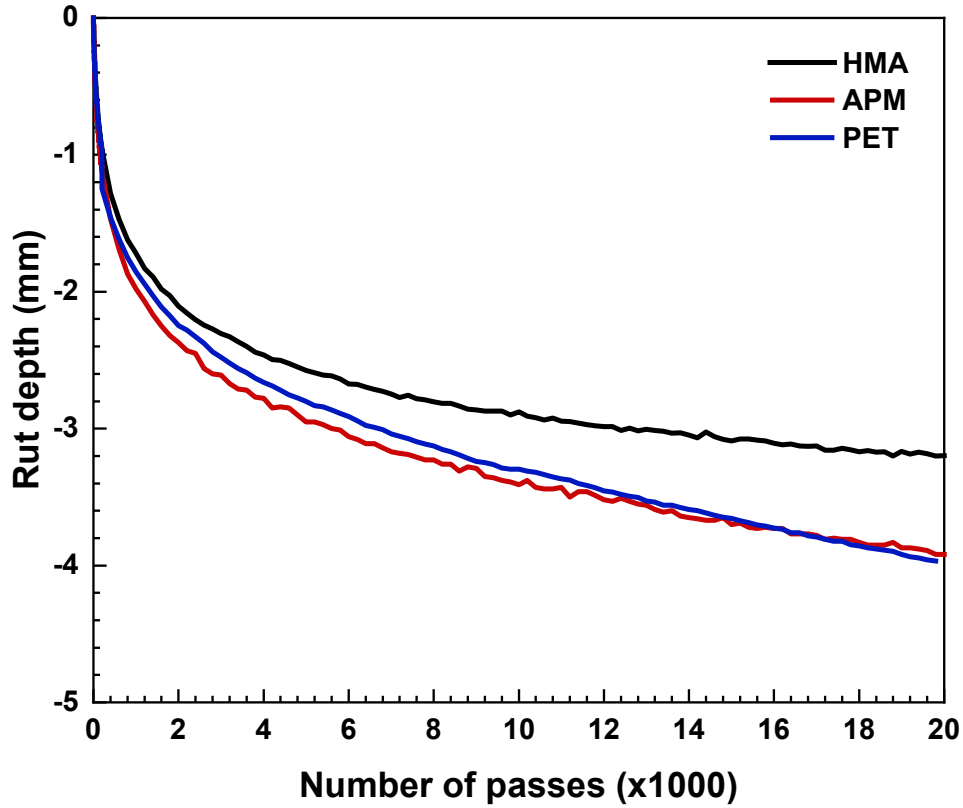
Fig. 10. IDT strengths of the produced asphalt mixtures

316 **3.4. Rutting resistance of the produced asphalt mixtures**

317 The following performance parameters are generally derived from the Hamburg wheel-tracking
 318 test, including creep slope, stripping slope, and stripping inflection point (SIP). The creep slope
 319 indicates the rutting resistance by the depth of rutting per loading pass in the creep stage. The
 320 stripping slope demonstrates the resistance to moisture damage by the rutting depth per loading
 321 pass in the stripping stage. SIP specifies the beginning of moisture damage, which is the number
 322 of passes that the regression lines of the creep stage and the stripping stage intersect.

323 **Fig. 11** shows Hamburg wheel-tracking results of HMA, PET, and APM at 50 °C. It is noticed that
324 the obtained curves only involved the creep stage throughout the 20,000 cycles of loading,
325 suggesting there was no distinct stripping developed during the test. The results indicated
326 satisfactory moisture damage resistances of the produced asphalt mixtures, which are consistent
327 with the findings of the moisture damage test. **Table 2** presents the measured values of creep slopes
328 and maximum rut depths of HMA, PET, and APM. After 20,000 cycles of loading, HMA showed
329 the lowest rut depth of 3.20 mm, while APM and PET had higher values of rut depths of 3.92 mm
330 and 3.97 mm. It is noted that the rutting resistance of asphalt mixtures decreases with the reduction
331 of production temperatures due to the deficient aging of the asphalt binder (Bennert et al., 2011).
332 Therefore, HMA mixtures are expected to perform better rutting resistances than WMA mixtures,
333 as the production temperatures of WMA mixtures were significantly lower than HMA mixtures.
334 The measured creep slopes and maximum rut depths of APM and PET were very close to each
335 other, which suggested that the use of aspha-min and PET-TETA had similar influences on the
336 rutting resistances of the produced asphalt mixtures. Although PET had strengthened molecular
337 bonding and stronger adhesive forces due to the asphalt binder modification, it seems that this
338 modification did not increase the rutting resistance of the produced asphalt mixture. A possible
339 reason is that PET-TETA is a soft polymer degraded from PET through the ammonolysis process,
340 it could improve the adhesion between asphalt binder and aggregate, but it might not be as effective
341 as in enhancing the cohesion of the modified asphalt binder. However, cohesion property is a
342 significant parameter in controlling the rutting performance of asphalt mixtures, especially in the
343 creep stage (Anderson et al., 1982; Kanitpong and Bahia, 2005). The findings suggest that the
344 application of PET-TETA had minimal influence on rutting resistance. A maximum rut depth of
345 0.5 in. (12.7mm) at 50 °C after 20,000 passes is allowed for asphalt mixtures prepared with a PG-

346 76 binder (Yildirim et al., 2007). It is clear that all three asphalt mixtures had sufficient rutting
 347 resistances, although APM and PET showed marginally higher maximum rut depths than HMA.



348

349 **Fig. 11.** Hamburg wheel-tracking curves of the produced asphalt mixtures

350

Table 2 Creep slope and the maximum rut depth of the produced asphalt mixtures

Mixture	Creep slope (mm/ 1000 passes)	Maximum rut depth (mm)
HMA	0.06	3.20
APM	0.09	3.92
PET	0.10	3.97

351 **4. Conclusions**

352 In this study, PET-TETA was synthesized using waste plastic bottles. Its chemical and physical
353 properties were characterized and compared with a commercial foaming additive. Then, three
354 asphalt mixtures (HMA, PET, and APM) were prepared, and their engineering performance was
355 investigated through comprehensive laboratory tests. The findings revealed that PET displayed
356 comparable performance to HMA and APM, with enhanced strength and resistance to elastic
357 deformation and stripping. This was attributed to the effective asphalt modification by PET-TETA.

358 In light of the above, the primary conclusions can be drawn as follows:

- 359 • The PET-TETA additive was characterized as a degraded polymer that consisted of both
360 amorphous and crystalline regions. The presence of hydration water was observed, which was
361 formed through hydrogen bonding between hydrophilic amide groups and water molecules.
362 Furthermore, it was found that the water molecules were predominantly attached to the
363 molecular chains in the amorphous regions due to space restrictions in the crystalline regions.
- 364 • PET-TETA generated superior asphalt foaming compared to the commercial foaming additive.
365 This was attributed to the higher content of hydration water present in PET-TETA, which was
366 approximately 60% greater than that of the commercial foaming additive.
- 367 • PET exhibited enhanced resistance to elastic deformation, as evidenced by its stiffness
368 modulus, which was approximately 15% higher than that of HMA and APM. However, further
369 investigation is required to evaluate its resistance to plastic deformation and fatigue cracking
370 after an extended period of service
- 371 • The use of PET-TETA as a foaming additive enhanced the coating between the asphalt binder
372 and the aggregate, resulting in an asphalt mixture that was more resistant to water stripping.

373 Additionally, PET exhibited improved strength properties than HMA and APM, with an
374 increase of approximately 13% and 23% observed prior to and after water conditioning,
375 respectively. PET also demonstrated the highest tensile strength ratio of 89.2% among the three
376 mixtures.

- 377 • All three asphalt mixtures exhibited satisfactory resistance to both rutting and moisture
378 damage. Nonetheless, PET and APM displayed slightly greater maximum rut depths than
379 HMA due to reduced aging of the asphalt binder at lower production temperatures.

380 The present study validated the effectiveness of applying PET-TETA as a foaming additive in
381 warm mix asphalt, offering a sustainable solution to the issue of waste plastic disposal by
382 producing a green paving material that utilizes waste plastic. In the future, a broader range of
383 asphalt mixtures will be prepared, and field investigations will be conducted to further validate the
384 performance of PET-TETA as a foaming additive. In addition, a life-cycle cost analysis of
385 incorporating PET-TETA in asphalt pavement will be included in future studies to provide a more
386 comprehensive understanding of the economic and environmental implications of this approach.

387 **Acknowledgments**

388 This work was supported by the Science and Technology Project of Henan Provincial
389 Department of Transportation (2020J6).

390

391 **References**

- 392 AASHTO, 2010. R30-02: Standard practice for mixture conditioning of hot mix asphalt (HMA).
393 *American Association of State Highway and Transportation Officials, Washington, D.C., United*
394 *States.*
- 395 AASHTO, 2013a. M320-10: Standard Specification for Performance-Graded Asphalt Binder.
396 *American Association of State Highway and Transportation Officials, Washington, D.C., United*
397 *States.*
- 398 AASHTO, 2013b. T324-11: Hamburg wheel-track testing of compacted hot mix asphalt (HMA).
399 *American Association of State Highway and Transportation Officials, Washington, D.C., United*
400 *States.*
- 401 Al-Hadidy, A. and Tan, Y.-Q., 2009. Mechanistic approach for polypropylene-modified flexible
402 pavements. *Materials & Design*, 30, 1133-1140.
- 403 Anderson, D. A., Dukatz, E. L. and Petersen, J. C. The effect of antistripping additives on the
404 properties of asphalt cement. *Association of Asphalt Paving Technologists Proceedings*, 1982.
- 405 ASTM, 2014. D4867-09: Standard test method for effect of moisture on asphalt concrete paving
406 mixtures. *American Society for Testing and Materials International, Pennsylvania, United*
407 *States.*
- 408 Awwad, M. T. and Shbeeb, L., 2007. The use of polyethylene in hot asphalt mixtures. *American*
409 *Journal of Applied Sciences*, 4, 390-396.
- 410 Bennert, T., Maher, A. and Sauber, R., 2011. Influence of production temperature and aggregate
411 moisture content on the initial performance of warm-mix asphalt. *Transportation research*
412 *record*, 2208, 97-107.
- 413 BSI, 1993. BS DD 213: Method for determination of the indirect tensile stiffness modulus of
414 bituminous mixtures. *British Standards Institution, London, U.K.*

415 Capitão, S., Picado-Santos, L. and Martinho, F., 2012. Pavement engineering materials: Review
416 on the use of warm-mix asphalt. *Construction and Building Materials*, 36, 1016-1024.

417 Duan, Y., Li, J., Yang, X., Hu, L., Wang, Z., Liu, Y. and Wang, C., 2008. Kinetic analysis on the
418 non-isothermal dehydration by integral master-plots method and TG–FTIR study of zinc acetate
419 dihydrate. *Journal of Analytical and Applied Pyrolysis*, 83, 1-6.

420 Hasan, M. R. M., You, Z., Porter, D. and Goh, S. W., 2015. Laboratory moisture susceptibility
421 evaluation of WMA under possible field conditions. *Construction and building materials*, 101,
422 57-64.

423 Highways Department, 2016. Guidance notes application of polymer modified stone mastic
424 asphalt. *Research & Development Division, RD/GN/038a*.

425 Hınıslioğlu, S. and Açar, E., 2004. Use of waste high density polyethylene as bitumen modifier
426 in asphalt concrete mix. *Materials letters*, 58, 267-271.

427 HK EPD, 2021. Monitoring of Solid Waste in Hong Kong 2020. *Hong Kong Environmental*
428 *Protection Department. Retrieved from*
429 <https://www.wastereduction.gov.hk/sites/default/files/msw2020.pdf>.

430 Jiang, J., Li, Y., Zhang, Y. and Bahia, H. U., 2022. Distribution of mortar film thickness and its
431 relationship to mixture cracking resistance. *International Journal of Pavement Engineering*, 23,
432 824-833.

433 Kanitpong, K. and Bahia, H., 2005. Relating adhesion and cohesion of asphalts to the effect of
434 moisture on laboratory performance of asphalt mixtures. *Transportation Research Record*, 1901,
435 33-43.

436 Leng, Z., Sreeram, A., Padhan, R. K. and Tan, Z., 2018. Value-added application of waste PET
437 based additives in bituminous mixtures containing high percentage of reclaimed asphalt
438 pavement (RAP). *Journal of cleaner Production*, 196, 615-625.

439 Li, R., Leng, Z., Wang, Y. and Zou, F., 2020. Characterization and correlation analysis of
440 mechanical properties and electrical resistance of asphalt emulsion cold-mix asphalt.
441 *Construction and Building Materials*, 263, 119974.

442 Li, R., Leng, Z., Yang, J., Lu, G., Huang, M., Lan, J., Zhang, H., Bai, Y. and Dong, Z., 2021.
443 Innovative application of waste polyethylene terephthalate (PET) derived additive as an
444 antistripping agent for asphalt mixture: Experimental investigation and molecular dynamics
445 simulation. *Fuel*, 300, 121015.

446 Liang, M., Xin, X., Fan, W., Zhang, J., Jiang, H. and Yao, Z., 2021. Comparison of rheological
447 properties and compatibility of asphalt modified with various polyethylene. *International*
448 *Journal of Pavement Engineering*, 22, 11-20.

449 Middleton, B. and Forfylow, R., 2009. Evaluation of warm-mix asphalt produced with the
450 double barrel green process. *Transportation research record*, 2126, 19-26.

451 Punith, V. and Veeraragavan, A., 2007. Behavior of asphalt concrete mixtures with reclaimed
452 polyethylene as additive. *Journal of materials in civil engineering*, 19, 500-507.

453 Rubio, M. C., Martínez, G., Baena, L. and Moreno, F., 2012. Warm mix asphalt: an overview.
454 *Journal of Cleaner Production*, 24, 76-84.

455 Saldo, J., Sendra, E. and Guamis, B., 2002. Changes in water binding in high-pressure treated
456 cheese, measured by TGA (thermogravimetric analysis). *Innovative Food Science & Emerging*
457 *Technologies*, 3, 203-207.

458 Sreeram, A., Leng, Z., Padhan, R. K. and Qu, X., 2018. Eco-friendly paving materials using
459 waste PET and reclaimed asphalt pavement. *HKIE Transactions*, 25, 237-247.

460 Tan, Z., Leng, Z., Jiang, J., Cao, P., Jelagin, D., Li, G. and Sreeram, A., 2022. Numerical study
461 of the aggregate contact effect on the complex modulus of asphalt concrete. *Materials & Design*,
462 213, 110342.

463 Xu, S., Xiao, F., Amirkhanian, S. and Singh, D., 2017. Moisture characteristics of mixtures with
464 warm mix asphalt technologies—A review. *Construction and Building Materials*, 142, 148-161.

465 Xu, X., Chen, G., Wu, Q., Leng, Z., Chen, X., Zhai, Y., Tu, Y. and Peng, C., 2022a. Chemical
466 upcycling of waste PET into sustainable asphalt pavement containing recycled concrete
467 aggregates: Insight into moisture-induced damage. *Construction and Building Materials*, 360,
468 129632.

469 Xu, X., Chu, Y., Chen, R., Wu, Q., Chen, X., Zou, F. and Peng, C., 2022b. Thermo-
470 mechanochemical recycling of waste polypropylene into degradation products as modifiers for
471 cleaner production and properties enhancement of bitumen. *Journal of Cleaner Production*,
472 134792.

473 Xu, X., Leng, Z., Lan, J., Wang, W., Yu, J., Bai, Y., Sreeram, A. and Hu, J., 2021. Sustainable
474 practice in pavement engineering through value-added collective recycling of waste plastic and
475 waste tyre rubber. *Engineering*, 7, 857-867.

476 Yeh, P. H., Nien, Y. H., Chen, J. H., Chen, W. C. and Chen, J. S., 2005. Thermal and rheological
477 properties of maleated polypropylene modified asphalt. *Polymer Engineering & Science*, 45,
478 1152-1158.

479 Yildirim, Y., Jayawickrama, P. W., Hossain, M. S., Alhabshi, A., Yildirim, C., Smit, A. D. F.
480 and Little, D., 2007. Hamburg wheel-tracking database analysis. *Texas Department of*
481 *Transportation and Federal Highway Administration, FHWA/TX-05/0-1707-7.*

482 Zhang, Y., Leng, Z., Zou, F., Wang, L., Chen, S. S. and Tsang, D. C., 2018. Synthesis of zeolite
483 A using sewage sludge ash for application in warm mix asphalt. *Journal of Cleaner Production,*
484 *172, 686-695.*

485 Zou, F., Leng, Z., Cao, R., Li, G., Zhang, Y. and Sreeram, A., 2022. Performance of zeolite
486 synthesized from sewage sludge ash as a warm mix asphalt additive. *Resources, Conservation*
487 *and Recycling, 181, 106254.*